Control and design of a hybrid energy storage system

Jérémy Dulout, Bruno Jammes, Lionel Séguier, Corinne Alonso

Control and design of a hybrid energy storage system

Jeremy Dulout[1,2], Bruno Jammes[1,2], Lionel Seguier[1], Corinne Alonso[1,2]
[1] CNRS, LAAS, 7 avenue du colonel Roche, F-31400 Toulouse, France
[2] Univ de Toulouse, UPS, LAAS, F-31400 Toulouse, France
E-Mail: jeremy.dulout@laas.fr - bruno.jammes@laas.fr

Keywords

«Battery Management Systems (BMS)», «Converter control», «DC power supply», «Energy Storage», «Supercapacitor».

Abstract

The increasing deployment of intermittent renewable energy sources (RESs) around the world has revealed concerns about the power grid stability. To solve this problem, a massive use of storage systems is needed. The main goal of this work is to develop a hybrid energy storage system (HESS) combining several storage devices with complementary performances. In this paper, lead-acid batteries and supercapacitors (SCs) are associated in order to deliver a pulsed current. An innovative cascade control with anti-windup tracking manages the power sharing between a buck and a boost converters connected to the same DC bus. Analog control circuits and power converters have been designed to evaluate the performances of the HESS in real conditions.

Introduction

Development of diversified energy sources is a world challenge in the struggle against pollution and energy costs reduction. Renewable energy sources (RESs) are more and more associated with energy storage systems (ESSs) to mitigate their high variability and unpredictable nature. More reliable distributed sources of energy are obtained thanks to ESSs [1-3]. Pumped hydro storage (PHS), compressed air energy storage (CAES), fuel cells, flywheels, batteries, supercapacitors (SCs) can be used to balance intermittent energy sources with different time scales, specific energy and power densities, costs... All these characteristics enable to optimize the ESS design, in terms of reliability and costs, for any application [4-7].

The Ragone plot (Fig.1) sums up different ESS's properties in terms of energy and power densities. Thus, a wise association of ESS with complementary characteristics could be an interesting solution to adapt HESS to any electrical load requirements with price and lifespan optimization.

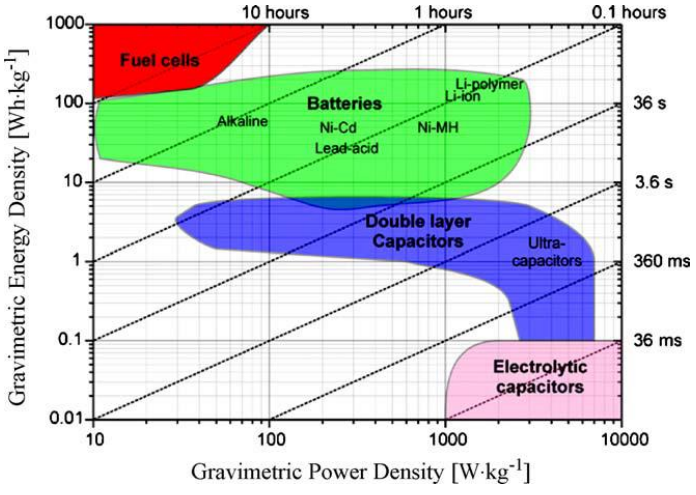

Fig. 1: The Ragone Plot with different ESS [8].

Different designs of HESSs and many power flow strategies are discussed in the literature [8-11]. In [12], it has been demonstrated that the performances and lifespan of ESSs, especially lead-acid batteries, can be reduced because of its operating conditions. Combining different ESSs can have a major impact on ageing mechanisms. For example, it has been proven that the lifetime of a lead-acid battery has increased by 30% when it is associated with SCs [13-14].

In this paper, a SC – lead-acid battery storage system is studied. Each unit is connected to a DC bus through a DC/DC converter. In our case, the battery unit has been chosen to provide a large energy density but its discharge current has been limited. SCs are used to deliver the remaining current when the battery's current reaches the limitation.

The first section of this paper introduces the concept of microgrid. A special attention is paid to storage systems and particularly electro-chemical ones. Next, the structure of the HESS is defined and the models of its components are presented. Then, the control strategy of the HESS is discussed and transfer functions of the converters are given. Finally, experimental results are provided.

Description of the global system

In this paper, the studied system is only a HESS associating two storage elements that create a DC bus on which is connected a DC load. The HESS is delivering a periodic pulsed current to the load. Such systems could be part of a microgrid (MG) as illustrated in Fig. 2. In this example, a photovoltaic source is connected to storage devices through different power static stages to supply AC or DC loads. MG is said to be on "connected mode" when it has a connection with a main distribution grid and "islanded mode" if not. A recent review has been done in [15].

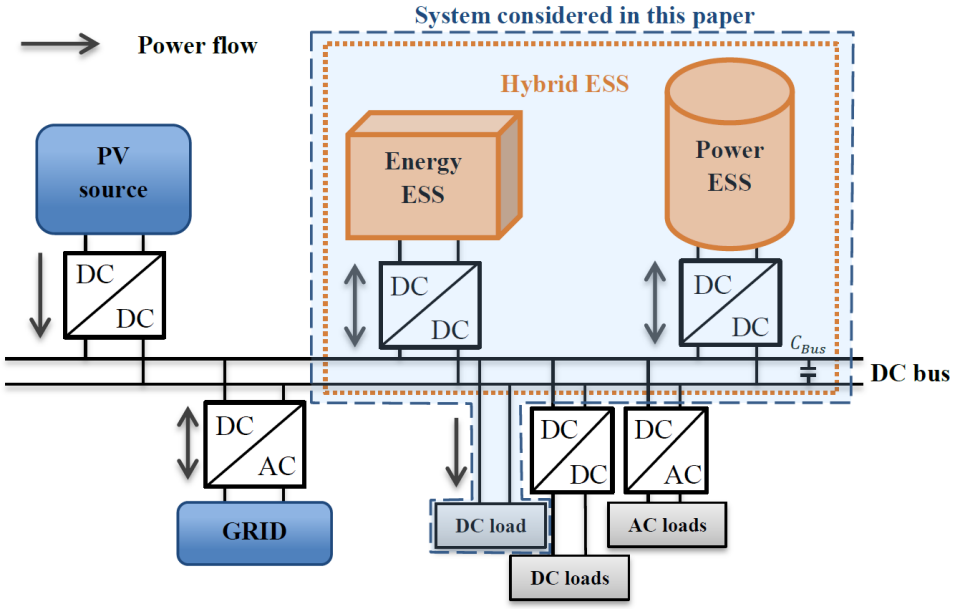

Fig. 2: Example of a microgrid with power flows.

We have a strong interest on the operating conditions of the electro-chemical storage systems. These devices have good performances when the charge and discharge currents are limited. Typically, manufacturers recommend to charge a lead-acid battery below a C/10 current (where C is the battery's nominal capacity) and to discharge the battery at a maximum current of C. These precautions allow to have available the nominal capacity of the battery and to keep a long lifetime.

A small scale experimental prototype has been built to evaluate the performances of our control algorithm. The DC bus voltage is regulated at 8V while a programmable DC electronic load generates current pulses. The typical current profile is described in Fig.3.

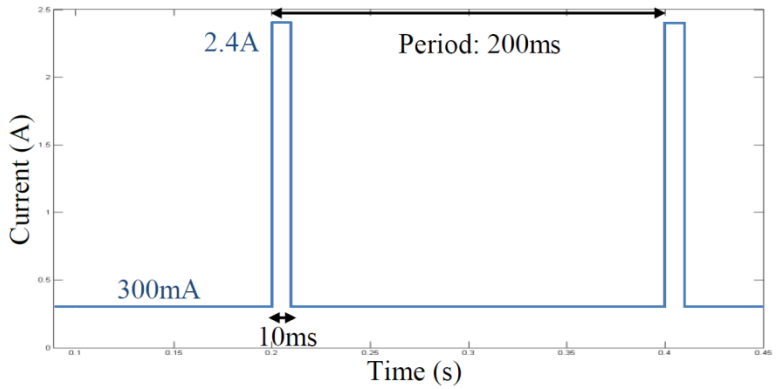

Fig. 3: Example of load's periodic current profile used to validate the HESS.

This HESS is working as a master-slave system. When the voltage of the bus is lower than the reference, the energy is drawn from the battery. If the battery's maximum current is reached, the remaining part of the current is delivered by the SC. In our case, 1A has been chosen as maximum discharge current which corresponds to the rated value of discharge current of our lead-acid battery. The HESS has been designed to supply the load during five seconds without recharging the SCs. In these conditions, two 10F-2,7V PowerStor® supercapacitors have been associated in series and two 1Ah-7V lead-acid batteries Yuasa® are connected in series.

We have chosen to use two current bidirectional DC/DC converters in order to allow charge and discharge of each ESS individually. Thus, the converters always operate in Continuous Conduction Mode (CCM). According to the voltage across the lead-acid module and the SCs, a buck converter is used to connect the battery to the DC bus and a boost converter connects the SCs to the DC bus.

Equivalent circuit modeling of the HESS

The structure of our HESS is depicted in Fig. 4. Several models of lead-acid battery and SC are studied as described in [8,13,14]. We choose to represent the battery by a constant voltage source with a constant internal resistor connected in series and the SC by a constant capacitor and a constant resistor in series. To precisely represent the DC/DC converters dynamics, we took into account equivalent series resistances (ESR) of inductors, capacitors and switches. The load imposes the current on the DC bus.

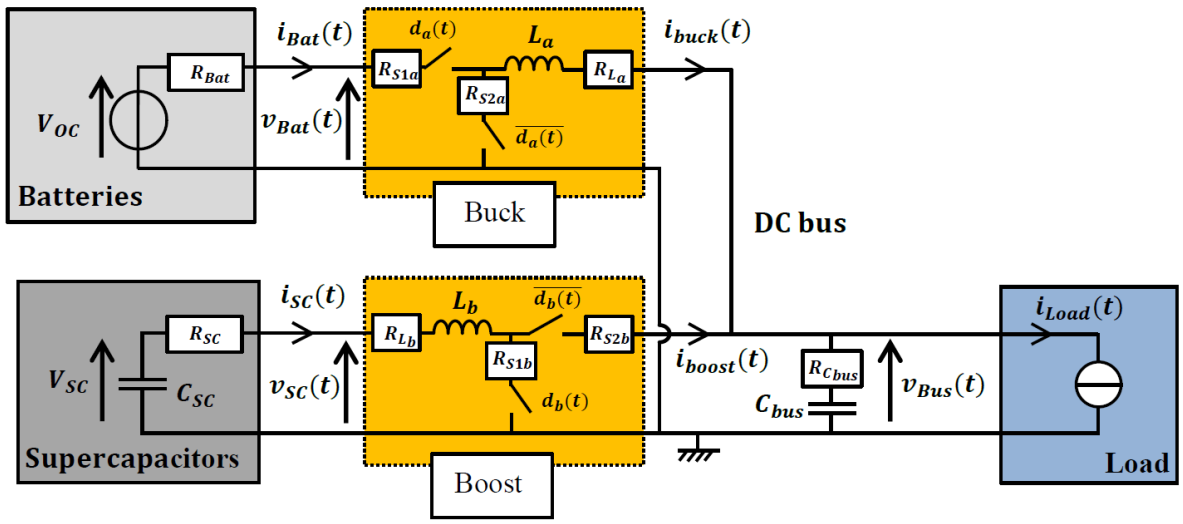

Fig. 4: Circuit model of the HESS connected to a DC load.

Table I: Nomenclature

C_{SC}	[F]	Nominal capacity of the SC's bank
C_{Bus}	[F]	Value of the capacitor on the DC bus
d_x(t)	dimensionless	Duty cycle of a converter
R_{Bat}	[Ω]	Battery's internal resistance
R_{L_x}/R_{Sx}/R_{SC}/$R_{C_{bus}}$	[Ω]	Inductor/Switch/SC/Capacitor's equivalent series resistance
V_{OC}	[V]	Open circuit voltage of battery
$i_{Load}(t)$	[A]	Current of the load
$i_{Bat}(t)/i_{SC}(t)$	[A]	Input currents of the buck/boost converter
$i_{buck}(t)/i_{boost}(t)$	[A]	Output currents of the buck/boost converter

Control strategy and transfer functions of the converters

The global control scheme of the HESS's converters is based on a standard cascade control (Fig. 5). The voltage loop (outer loop) regulates the voltage of the bus and determines the references of currents of the two converters (inner loops). The regulation is done on the averaged input currents of the two converters which are obtained with a low-pass filter (with a cut-off frequency of 100kHz). Only the buck converter is working until the maximum current that the battery can deliver is reached. Beyond, the two converters are working together to keep 8V on the DC bus. We have used three PI controllers because they are easy to tune, eliminate disturbances and give appropriate responses.

According to the nominal operating conditions of a lead-acid battery, the current of the buck converter is limited to 1A. We also limited the current of the boost converter to avoid too large currents that may damage it. The duty cycles are also saturated in order to take into account real component's switching time. These limitations introduce nonlinear effects that may change significantly the system behavior or even worse, make it unstable. Indeed, when limitations are reached, the integrating action of the controller is growing and can take a very large value. This means that even if the sign of the error changes, the effect on the output of the controller can take a very long time. This phenomenon is called integrator windup. Among the several anti-windup strategies proposed in [16] and [17], we have chosen to use the tracking method. This method allows to act on the overshoot and settling time of the system by changing the feedback gain of the anti-windup mechanism. A large value of integrating action is prevented because when a limitation is reached, the anti-windup feedback keeps the input of the integrator in a reduced scale. The anti-windup feedback gain is comprised between 0 and the gain of the integrating action. Having a feedback gain close to the gain of the integrating action will reduce the overshoot but will increase the settling time. For this application, we have chosen a gain equals to the gain of the integrating action. The PI controllers and anti-windup strategy are represented in light grey areas in Fig. 5.

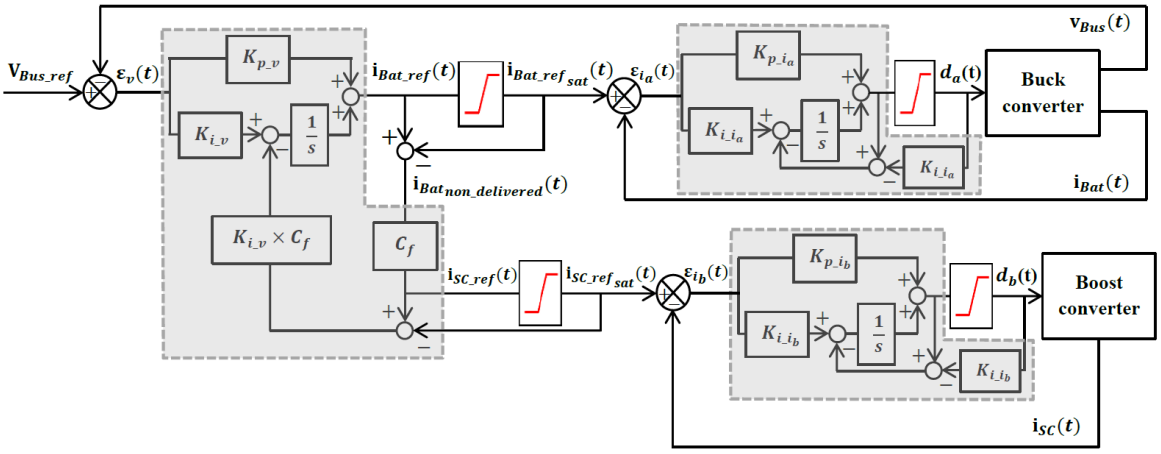

Fig. 5: Control scheme of the HESS.

By linearizing the averaged equations of the converters over a switching time period and around a steady state operating point we get the HESS's average small signal model. For any signal x(t), $\tilde{x}$ is a small variation of x(t) around the nominal value X. The transfer functions of the converters are given by (Eq. 1.b), (Eq. 2.b) and (Eq. 3). For the design of the current loops regulators, we assume that $v_{Bus}(t)$ is constant (its dynamic is very slow compared to the current's dynamic). The regulation of the input current of the buck converter is not commonly used, but it is necessary in our case to deal with the nominal operating conditions of the battery.

By neglecting the variations of the input voltage, we find the following transfer function between $\widetilde{I_{Bat}(s)}$ and $\widetilde{D_a(s)}$ which are respectively the Laplace transform of the input current and the duty cycle of the buck converter:

$$\frac{\widetilde{I_{Bat}(s)}}{\widetilde{D_a(s)}} = \frac{L_a I_{buck}\, s + D_a\, V_{oc} + (R_{S2a} + R_{L_a})\, I_{buck} - (R_{Bat} + R_{S1a}) D_a I_{Bat}}{L_a\, s + (1 - D_a) R_{S2a} + R_{L_a} + (R_{Bat} + R_{S1a})\, D_a} \qquad \text{(Eq. 1.a)}$$

Where s is the Laplace variable.

Assuming that $R_{Bat} \gg R_{S1a}$, $R_{L_a} \gg R_{S2a}$ and $R_{L_a} I_{buck} \approx R_{Bat} D_a I_{Bat}$ we can simplify the previous transfer function:

$$\frac{\widetilde{I_{Bat}(s)}}{\widetilde{D_a(s)}} = \frac{L_a I_{buck}\, s + D_a\, V_{oc}}{L_a\, s + R_{L_a} + R_{Bat}\, D_a} \qquad \text{(Eq. 1.b)}$$

By neglecting the variations of the input voltage, we can write:

$$\frac{\widetilde{I_{SC}(s)}}{\widetilde{D_b(s)}} = \frac{V_{bus} - R_{S1b} I_{SC}}{L_b s + D_b R_{S1b} + R_{SC} + R_{L_b} + (1 - D_b)^2 R_{S2b}} \qquad \text{(Eq. 2.a)}$$

Assuming that $R_{SC} \gg R_{S1b}$ and $R_{SC} \gg R_{S2b}$ we can simplify the previous transfer function:

$$\frac{\widetilde{I_{SC}(s)}}{\widetilde{D_b(s)}} = \frac{V_{bus}}{L_b s + R_{SC} + R_{L_b}} \qquad \text{(Eq. 2.b)}$$

Then, we have defined the transfer function of the bus voltage, considering that the current is only delivered by the buck converter:

$$\frac{\widetilde{V_{Bus}(s)}}{\widetilde{I_{Bat}(s)}} = \frac{R_{C_{bus}} C_{bus}\, s + 1}{D_a\, C_{bus}\, s} \qquad \text{(Eq. 3)}$$

We also looked at the transfer function of the bus voltage, considering that the current is only delivered by the boost converter:

$$\frac{\widetilde{V_{Bus}(s)}}{\widetilde{I_{SC}(s)}} = \frac{(1 - D_b)\, R_{C_{bus}} C_{bus}\, s + 1 - D_b}{C_{bus}\, s} \qquad \text{(Eq. 4)}$$

From (Eq.3) and (Eq.4), we can also write:

$$\frac{\widetilde{V_{Bus}(s)}}{\widetilde{I_{Bat}(s)}} = \frac{1}{D_a(1 - D_b)} \frac{\widetilde{v_{Bus}}}{\widetilde{i_{SC}}} = C_f \frac{\widetilde{v_{Bus}}}{\widetilde{i_{SC}}} \qquad \text{(Eq. 5)}$$

where C_f is a dimensionless factor.

PI controllers have been designed using the classical phase margin method. We chose large bandwidths to obtain fast settling times: 70 000rad/s for current loops and 7 000rad/s for voltage loop. As a rule of thumb, the inner loop's dynamic of cascade control has to be around ten times faster than the outer loop's dynamic. We set the phase margin around 60° which is supposed to give the best trade-off between system response and overshoot.

For the voltage regulation, we designed a PI controller based on (Eq. 3). To determine the proper reference of the current loop of the boost, we insert the factor C_f (Eq. 5) at the output of the controller as depicted in Fig. 5.

Experimental results

The system parameters are summarized in table II.

Table II: System parameters

Parameters	Minimum	Maximum
Battery voltage	11.5V	14V
SC's pack voltage	3.6V	5.4V
Bus voltage	7V	9V
Iload(t)	300mA	2.1A
Switching frequency	250kHz	
$R_{Bat}/R_{SC}/R_{L_a}/R_{L_b}/R_{C_{Bus}}$	0,04Ω/0.02Ω/0.05Ω/0.05Ω/0.02Ω	
$L_a/L_b/C_{Bus}$	240µH/190,4µH/500µF	
$K_{P\_v}/K_{i\_v}/K_{P\_i_a}/K_{i\_i_a}/K_{P\_i_b}/K_{i\_i_b}$	1.8/7720/2.3/28750/1.5/21884	

First, the system has been simulated with Scilab-Xcos. The results are summarized in Fig. 6. The duration of the current's load pulses has been reduced to have a good overview of voltage and current dynamics.

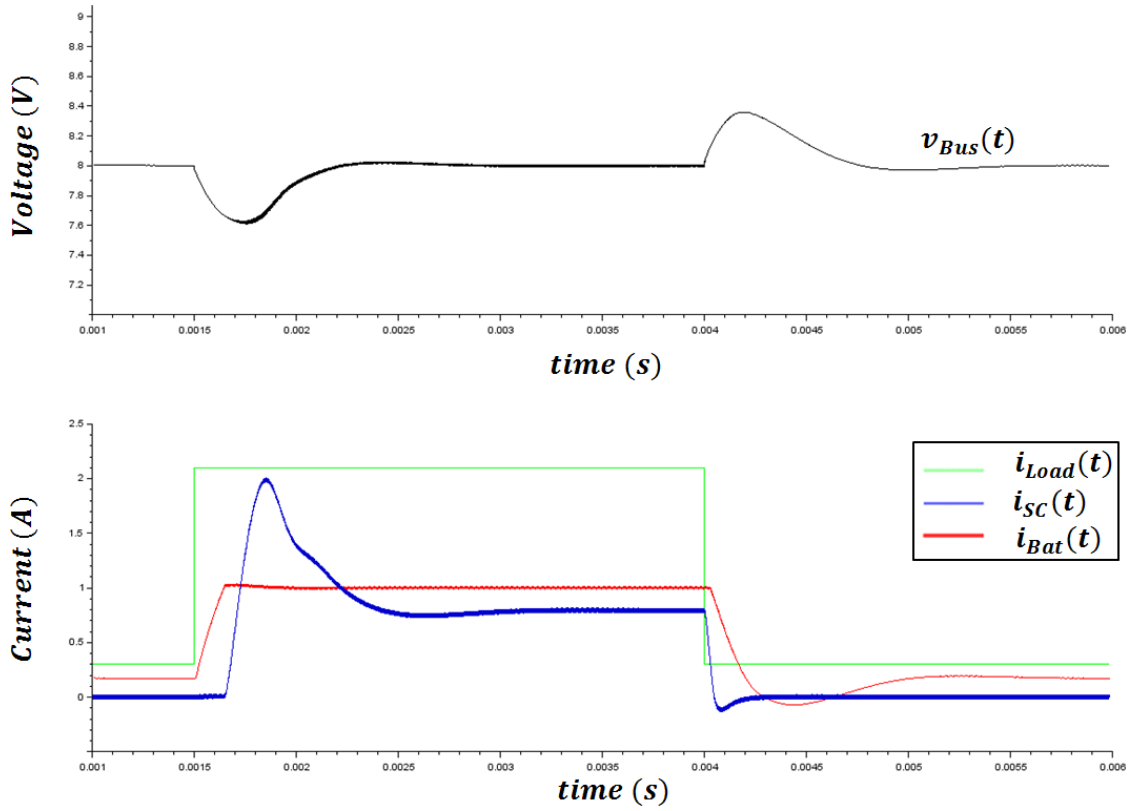

Fig. 6: Simulation results with Scilab-Xcos (step of load's current from 0.3A to 2.1A).

In Fig. 6, the current and voltage responses match with the specifications: when the load current is high (2.1A), the battery current is limited to 1A and the SC delivers the remaining current to regulate the DC bus. The voltage's variations are lower than 0.5V.

For such levels of currents, we have noticed that anti-windup is not needed (the duty cycles and the current of the boost converter do not reach their limitations). The anti-windup strategy will only be useful for high current pulses. In consequence, we have chosen to not implement any anti-windup strategy on our experimental control board. Besides, to implement an anti-windup strategy on an analog control board, several additional operational amplifiers would be needed.

In order to experiment our control strategy, we have designed a buck and a boost converters. A control board has also been designed. As no charging strategy for the battery and SC has been implemented, we have designed unidirectional converters.

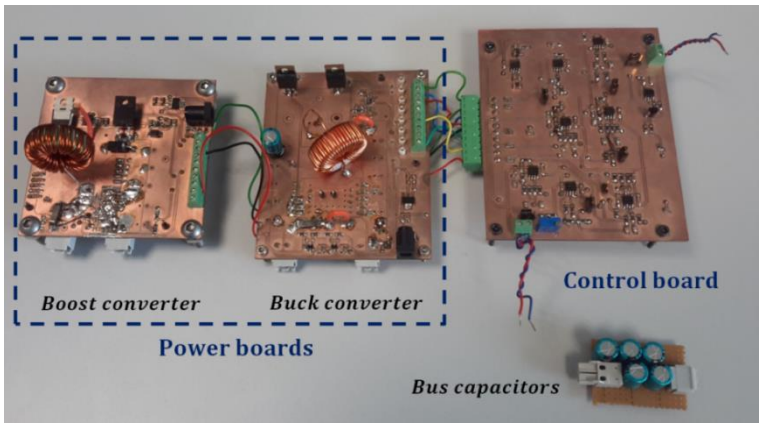

Fig. 7: actual experimental study.

The experimental results (Fig. 8) are similar to the simulations, except the bus voltage drop which is more important in real conditions than in simulations. In normal conditions, when the current reference of the boost is 0, the duty cycle should be around 60%. But due to an offset on the current sensor of the boost converter, the duty cycle reaches its minimum value.

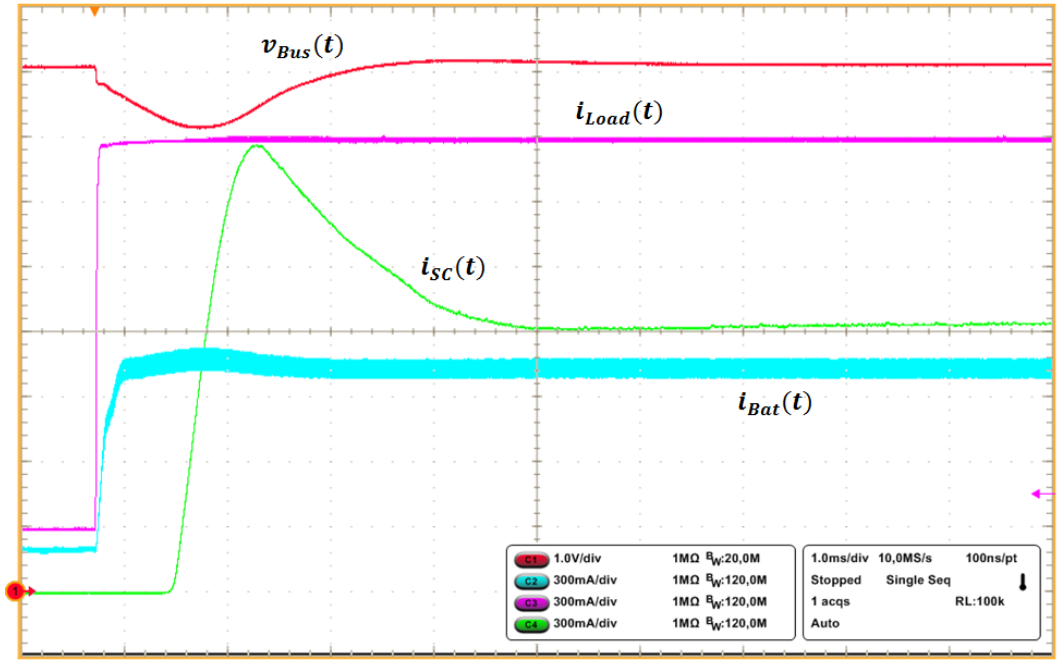

Fig. 8: System's response, experimental results (step of load's current from 0.3A to 2.1A).

Unless the current loop is very fast, the duty cycle needs a "long" time to reach the right value from 0 (Fig. 9). The noise on the current reference of the boost converter ($\mathbf{i}_{SC_{ref}}(t)$ on Fig. 9) is the consequence of the operational amplifiers of the circuit used to saturate the current reference of the buck converter.

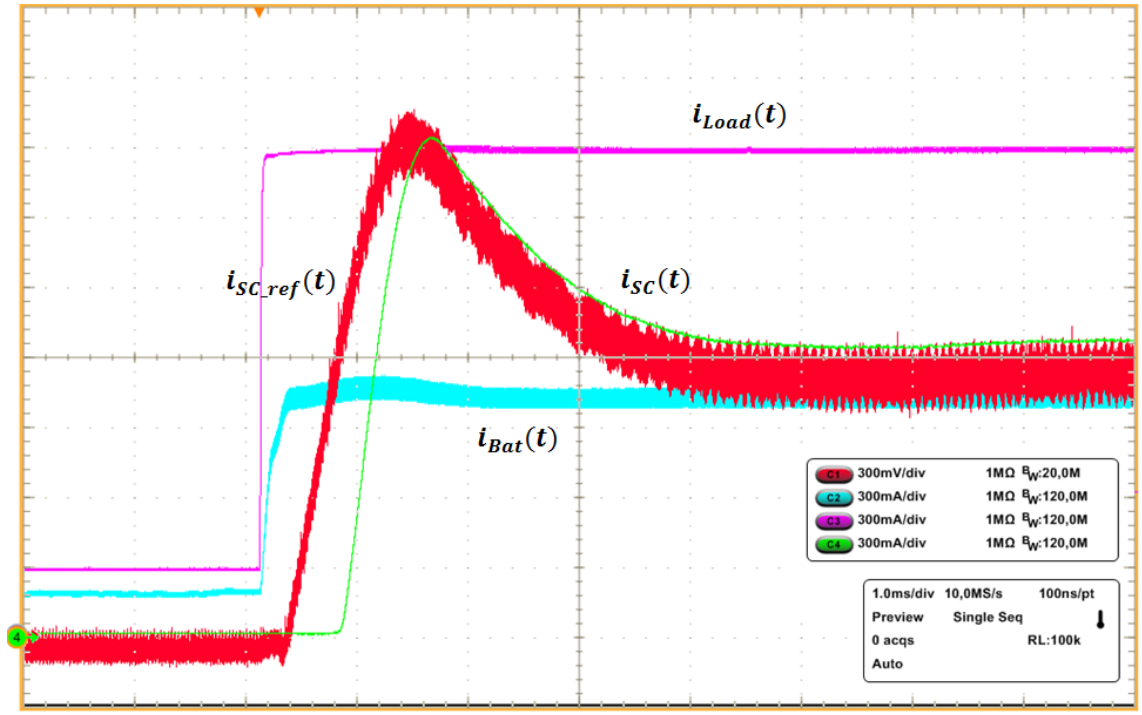

Fig. 9: Delay on the boost converter (step of load's current from 0.3A to 2.1A).

Clearly, this delay does not exist when the duty cycle of the boost converter at the initial conditions is not at the minimum value (Fig. 10).

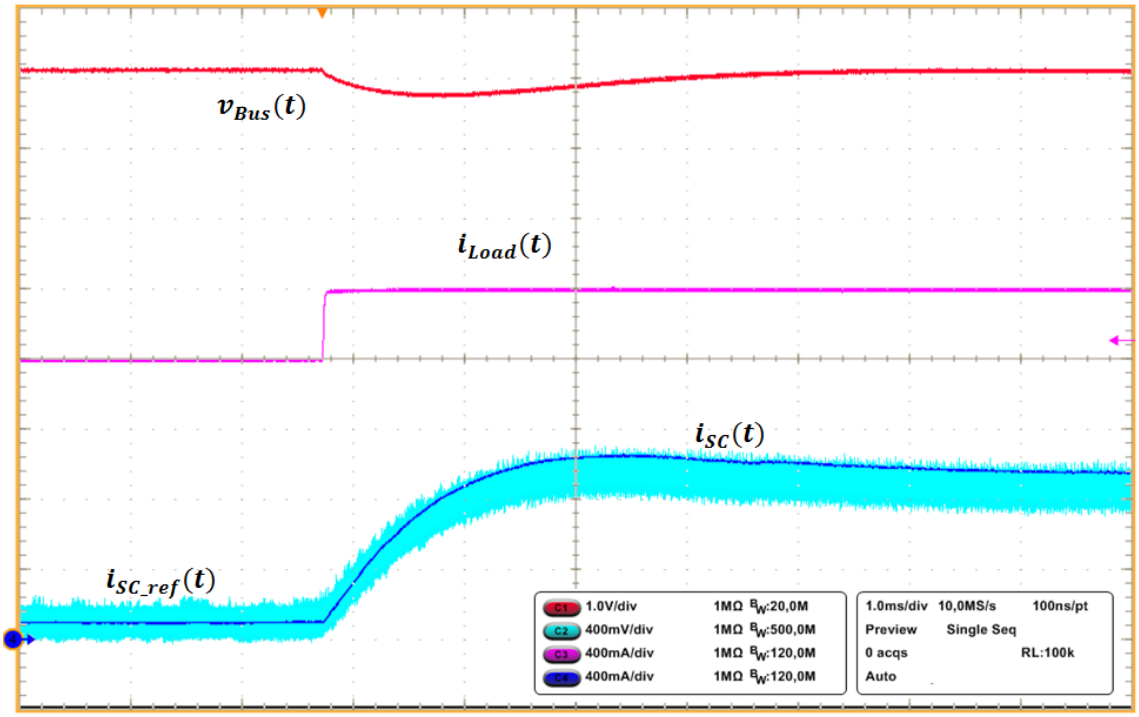

Fig. 10: No delay on the boost converter (step of load's current from 1.6A to 2A).

Conclusion

This paper proposes the design and the control strategy of a SC – lead-acid battery HESS adapted to pulsed current loads. The goal of this control scheme is to use each elementary ESS in optimal conditions of use. In our case, the aim of the hybridization is to increase the lifetime of a lead-acid battery by using it under its nominal conditions (the current of the battery has been limited).

Average small signal models of the two converters delivering a pulsed current are presented in this paper. Cascade control and anti-windup tracking has been implemented. It enables to limit the discharge current of the battery in order to respect the constraints for a high lifetime of a lead-acid battery. When high discharge currents are necessary to maintain the bus voltage at the reference, the SCs are delivering the remaining part of the current.

Finally a HESS delivering a pulsed current has been built (power and control boards). Simulations and experimental results validate our approach.

In the future, other energy sources have to be included to the system in order to study the stability of a microgrid which combines a large number of sources. A digital control may be implemented to have a better flexibility and easily experiment different control strategies.

References

[1] Jayasekara N., Wolfs P., Masoum M.A.S.: An optimal management strategy for distributed storages in distribution networks with high penetrations of PV, Electric Power Systems Research 116 (2014) 147-157.
[2] Moraes Toledo O., Oliveira Filho D., Alves Cardoso Diniz A.S.: Distributed photovoltaic generation and energy storage systems: A review, Renewable and Sustainable Energy Reviews 14 (2010) 506-511.
[3] Beaudin M. & al.: Energy storage for mitigating the variability of renewable electricity sources: An updated review, Energy for Sustainable Development 14 (2010) 302-314.
[4] Ibrahim H., Ilinca A., Perron J.: Energy storage systems-Characteristics and comparisons, Renewable and Sustainable Energy Reviews 12 (2008) 1221-1250.
[5] Chen H. & al.: Progress in electrical energy storage system: A critical review, Progress in Natural Science 19 (2009) 291-312.
[6] Kouskou T. & al.: Energy storage: Applications and challenges, Solar Energy Materials & Solar Cells 120 (2014) 59-80.
[7] Koohi-Kamali S. & al.: Emergence of energy storage technologies as the solution for reliable operation of smart power systems: A review, Renewable and Sustainable Energy Reviews 25 (2013) 135-165.
[8] Kuperman A., Aharon I.: Battery-ultracapacitor hybrids for pulsed current loads: A review, Renewable and Sustainable Energy Reviews 15 (2011) 981-992.
[9] Curti J.M.A. & al.: A simplified Power Management Strategy for a Supercapacitor/Battery Hybrid Energy Storage System using the Half-Controlled Converter, IECON 2012 – 38th Annual Conference on IEEE Industrial Electronics Society, 4006-4011.
[10] Jung H., Wang H., Hu T.: Control design for robust tracking and smooth transition in power systems with battery/supercapacitor hybrid energy storage devices, Journal of Power Sources 267 (2014) 566-575.
[11] Thounthong P., Raël S., Davat B.: Control Strategy of Fuel Cell and Supercapacitors Association for a Distributed Generation System, IEEE Transactions On Industrial Electronics, Vol. 54, No. 6, december 2007, 3225-3233.
[12] Ruetschi P.: Aging mechanisms and service life of lead-acid batteries, Journal of Power Sources 127 (2004) 33-44.
[13] Omar N. & al.: Power and life enhancement of battery-electrical double layer capacitor for hybrid electric and charge-depleting plug-in vehicle applications, Electrochimica Acta 55 (2010) 7524-7531.
[14] Dougal R.A., Liu S., White R.E.: Power and Life Extension of Battery-Ultracapacitor Hybrids, IEEE Transactions On Components And Packaging Technologies, Vol. 25, No. 1, march 2002, 120-131.
[15] Justo J.J., Mwasilu F., Lee J., Jung J.-W.: AC-microgrids versus DC-microgrids with distributed energy resources: A review, Renewable and Sustainable Energy Reviews 24 (2013) 387-405.
[16] Bohn C., Atherton D.P., A SIMULINK package for comparative studies of PID anti-windup strategies, IEEE/IFAC Joint Symposium on Computer-Aided Control System Design, 1994, 447-452.
[17] Aström K.J., Hägglund T.: PID controllers: theory, design and tuning, Instrument Society of America, 1995.